

DEVELOPMENT OF FPGA-BASED PREDISTORTION-TYPE LINEARIZATION ALGORITHMS FOR KLYSTRONS WITHIN DIGITAL LLRF CONTROL SYSTEMS FOR ILC-LIKE ELECTRON ACCELERATORS

M. Omet*, SOKENDAI, Hayama, Japan

S. Michizono, T. Matsumoto, T. Miura, F. Qiu, KEK/SOKENDAI, Tsukuba, Japan

B. Chase, P. Varghese, FNAL, Batavia, USA

Abstract

Two different kinds of predistortion-type linearization algorithms have been implemented and compared on an FPGA within the digital LLRF control system the Advanced Superconducting Test Facility (ASTA) at the Fermi National Accelerator Laboratory (FNAL). The algorithms are based on 2nd order polynomial functions and lookup tables with interpolation by which complex correction factors are obtained. The algorithms were tested in an actual setup including a 5 MW klystron and a superconducting 9-cell TESLA-type cavity at ASTA. By this a proof of concept was demonstrated.

INTRODUCTION

At the International Linear Collider (ILC) [1] the superconducting cavities of the main linacs will be controlled using digital low level radio frequency (LLRF) techniques [2]. Figure 1 shows a schematic of a typical LLRF control loop. The from the cavity picked up radio frequency (RF) is down converted in frequency by mixing with the local oscillator (LO) signal. The resulting signal, the intermediate frequency (IF), is digitized using an analog-to-digital converter (ADC). The digital signal is processed on an FPGA, which contains beside others the controller. The processed signal is converted from digital to analog. The analog signal is fed beside an RF signal to an IQ modulator for up conversion in frequency. The resulting RF signal is amplified by a klystron, which drives the cavity. In case of ILC groups of 39 cavities will be driven by single 10 MW multi-beam klystrons.

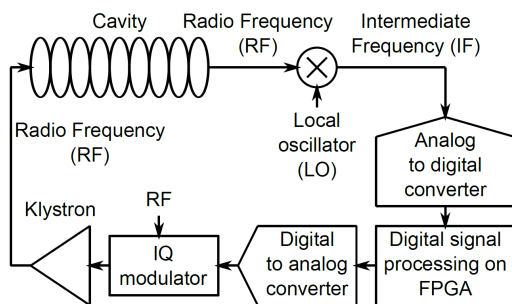


Figure 1: Schematic of a typical digital LLRF control loop.

Typically the input-to-output characteristics of a klystron in both amplitude and phase are not linear. A schematic of

a typical input-to-output characteristics is shown in Figure 2 in black. In order to operate the klystrons at ILC most cost effectively, it is intended to operate them 7% in power below the point of saturation. At this point the slope of the input-power-to-output-power characteristics is only about $\frac{1}{10}$ compared to the slope at the linear region. Since the control gain is proportional to this slope, it also degrades close to the point of saturation. In order to keep the feedback effective, it is required to keep the amplitude slope constant and the phase rotation at 0° until the point of saturation. The desired klystron output is shown in Figure 2 in red. This can be accomplished by using a klystron linearization. The linearization algorithms described in the following are predistortion-type linearizations, implemented in the firmware of the field programmable gate array (FPGA), on which beside others the digital LLRF controller is located. The predistortion characteristics are inverse to the non-linear characteristics of the klystron. The predistorter is typically located after the controller and the addition of feedforward tables and before transmitting the signals to the digital-to-analog converters (DACs). The predistortion is generated in dependency of the signal amplitude. In the past linearization concepts were already implemented [3, 4]. The studies described in the following are based on those.

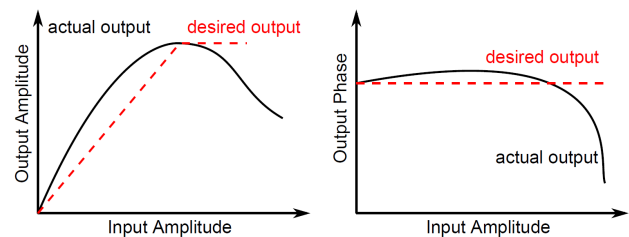


Figure 2: Schematic of the klystron amplitude and phase output characteristics.

KLYSTRON LINEARIZATION ALGORITHM IMPLEMENTATION

At FNAL ASTA [5] is under construction. Since it is beside an user machine also an ILC R&D accelerator, the digital LLRF control system was designed with ILC in mind.

In the presented study two kinds of predistortion-type amplitude dependent klystron linearization algorithms were implemented and tested. The target hardware was an Altera Cyclone II FPGA on the multi-cavity field control (MFC)

* momet@post.kek.jp

module [6]. The first algorithm implemented was a redesign based on a formerly implemented algorithm for the linearization of the amplitude only [4]. With the redesign the support of phase linearization was added. Its principle is based on

$$\begin{pmatrix} I_{out} \\ Q_{out} \end{pmatrix} = \begin{pmatrix} f_i(A) & -f_q(A) \\ f_q(A) & f_i(A) \end{pmatrix} \begin{pmatrix} I_{in} \\ Q_{in} \end{pmatrix}, \quad (1)$$

where $f_i(A)$ and $f_q(A)$ are 2nd order polynomial functions. In Figure 3 the schematic of the implemented algorithm is shown. From the I_{in} and Q_{in} input values the amplitude A is computed. Based on this I and Q correction factors are calculated by two 2nd order polynomial functions. The computed I and Q correction factors are applied to the input I_{in} and Q_{in} values using a complex multiplication realized by four multipliers, one subtractor, and one adder. From the corrected I_{in} and Q_{in} values the amplitude B is computed and compared to a predefined limit ($limit$). If the amplitude exceeds the limit, a correction factor $f_{corr,l} = \frac{limit}{B}$ is applied. If the limit is not exceeded, the the correction factor $f_{corr,l} = 1$ is applied, leaving the corrected I_{in} and Q_{in} unchanged. By two switches the linearized and amplitude limited or the original I_{in} and Q_{in} values can be chosen as the output I_{out} and Q_{out} .

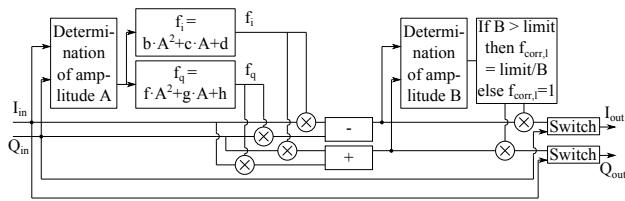


Figure 3: Schematic of second order polynomial-based klystron linearization algorithm.

In the case of the second linearization algorithm implemented the correction is also based on equation (1), but in this case $f_i(A)$ and $f_q(A)$ are created by lookup tables with interpolation [7]. The lookup table with interpolation-based algorithm consists of two lookup tables (four 12-bit lookup tables for the final implementation). In the first lookup table (LUT1 and LUT3) the nodes y_n are stored, similar to the case of a direct lookup table [4]. In the second lookup table (LUT2 and LUT4), the slopes between the nodes m_n calculated by the differential quotient are stored. The output value of the algorithm y is calculated by

$$y = y_n + \Delta x \cdot m_n, \quad (2)$$

where $\Delta x = A - x_n$. A is the input value amplitude A and x_n the to the node y_n corresponding x value. Figure 4 shows a schematic of the implementation of the klystron linearization algorithm. Since a complex correction factor is generated, the lookup table with interpolation algorithm is implemented two times. The correction factors f_i and f_q are individually computed corresponding to y in equation (2). Beside the change of the method of the generation of the complex correction factor, the signal flow is the same as

described previously for the klystron linearization based on two 2nd order polynomial functions.

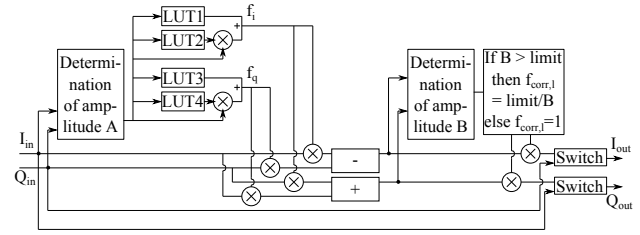


Figure 4: Schematic of the lookup table with interpolation-based klystron linearization package.

In Table 1 the clock cycles required for the execution of the linearization algorithms and for the execution of the amplitude limitations are compared. The for this required time does not effect the total loop delay, because all computations are performed in a parallel process. The loop delays added due to the application of the linearization algorithms are also listed in Table 1. The Altera Cyclone II on which the algorithms were implemented is clocked at a frequency of 62.5 MHz.

Table 1: Comparison of Required Computation Times

Algorithm	Lin. [clk. cyc.]	Limiter [clk. cyc.]	Add. loop del. [clk. cyc.]
2nd order	20	19	3
LUT w/int.	19	19	3

The computation times are dominated by the computation of the amplitude using the square root block, which is pipelined with 12 clocks. The algorithm with the shortest computation time is the one based on the lookup tables with interpolation.

TEST OF ALGORITHMS

The two linearization algorithms implemented at FNAL were tested at ASTA. In preparation for the test of the klystron linearization algorithm a klystron characterization was conducted. To this end under open loop operation of the klystron a feedforward (FF) amplitude scan over the whole range possible from 0 to 1 [a.u.] was performed. The klystron output characteristics in terms of amplitude, square root of the output power, and phase were recorded. Based on this the parameters and lookup tables for both linearization algorithms were computed.

Figure 5 shows the klystron output amplitude versus the FF amplitude during characterization and in the case of no linearization active in yellow. The same figure shows also the klystron output amplitudes in case the two linearization algorithms were active (blue for the 2nd order polynomial-based and purple for the lookup table with interpolation-based). The target amplitude characteristic is plotted in green. It can be seen that the 2nd order polynomial function-

based klystron linearization has the better linearization performance concerning the amplitude.

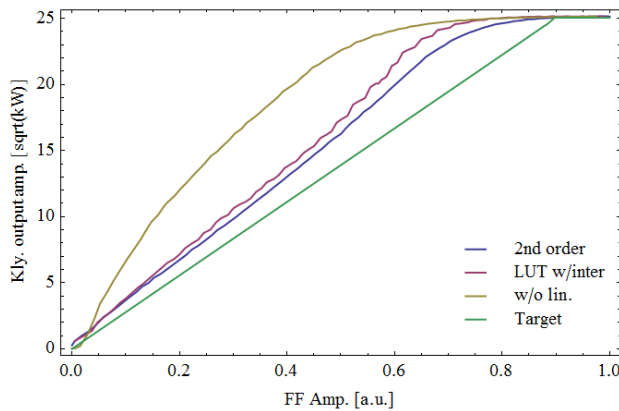


Figure 5: Klystron output amplitude [$\sqrt{\text{kW}}$] versus FF amplitude [a.u.]: 2nd order polynomial function-based linearization (blue), and with LUT with interpolation-based linearization (purple), without linearization (yellow), target amplitude (green).

Figure 6 shows the klystron output phase for the case no linearization was active in yellow as well as the target phase characteristic in green. In this case the maximal phase rotation was 40° . In the same figure the also the phases during the 2nd order polynomial function-based (blue) and the lookup table with interpolation-based (purple) algorithms were active are shown. It can be seen that the lookup table with interpolation-based klystron linearization algorithm has the best linearization performance concerning the phase with 13° over the whole FF amplitude range. For the FF amplitude range until the point of saturation the phase rotation is with only 5° even lower. The maximal phase rotation of the 2nd order polynomial function-based algorithm was 15° .

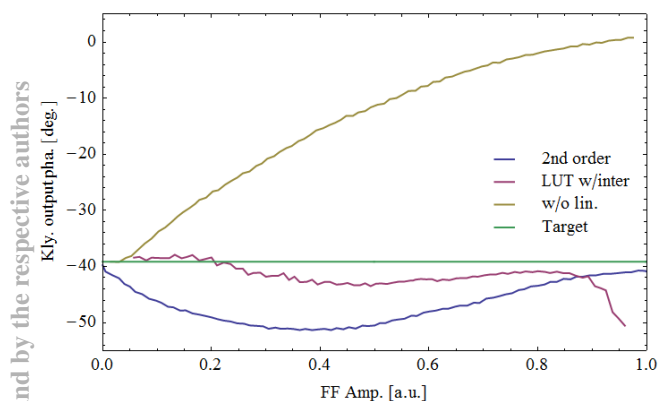


Figure 6: Klystron output phase [$^\circ$] versus FF amplitude [a.u.]: 2nd order polynomial function-based linearization (blue), and with LUT with interpolation-based linearization (purple), without linearization (yellow), target phase (green).

The fluctuations and deviations to the target functions in amplitude and phase in the case of the lookup table with interpolation-based algorithm originate from an error regarding the computation of the slope lookup tables. The deviations of the 2nd order polynomial function-based algorithm originate from not sufficiently optimized configuration parameters ($b, c, d, f, g,$ and h). Nevertheless with the presented data a prove of concept of both the 2nd order polynomial function-based and the lookup table with interpolation-based linearization algorithms was demonstrated.

SUMMARY

At FNAL linearization algorithms based on two 2nd order polynomial functions and lookup tables with interpolation were implemented. In both cases the quantization of the output of the linearization algorithm was avoided. In the cases of the polynomial function-based algorithm furthermore the memory requirements could be reduced drastically, since only few configuration parameters had to be stored instead of lookup tables. Both algorithms were tested using a 5 MW klystron at FNAL ASTA resulting in a prove of concept. Within both implemented and tested algorithms the one based on lookup tables with interpolation yields theoretically the best linearization performance.

The described linearization technique is not only suitable for ILC but is also for other accelerators and applications at which high efficiency RF usage is required.

REFERENCES

- [1] <http://www.linearcollider.org>
- [2] "The International Linear Collider – Technical Design Report – Volume 3.II: Accelerator Baseline Design", CERN, FNAL, KEK (2013).
- [3] W. Cichalewski, "Linearization of Microwave High Power Amplifiers Chain in the RF Systems of Linear Accelerators for FLASH and X-FEL" (PhD Thesis), Technical University of Lodz, Lodz (2008).
- [4] M. Omet, "Development and Test of Klystron Linearization Packages for FPGA-based Low Level RF Control Systems of ILC-like Electron Accelerators", Proc. RT2014, Nara (2014).
- [5] <http://asta.fnal.gov/>
- [6] P. Varghese, "Multi-cavity Field Control (MFC) Module Description", FNAL, Batavia (2009).
- [7] B. Chase, private communication, FNAL, Batavia (2014).